

Iso-Diffusion: Improving Diffusion Probabilistic Models Using the Isotropy of the Additive Gaussian Noise

Dilum Fernando¹, Dhanajaya Jayasundara², Roshan Godaliyadda¹, Chaminda Bandara³, Parakrama Ekanayake¹, and Vijitha Herath¹

¹ University of Peradeniya, Peradeniya, Sri Lanka

² Johns Hopkins University, Baltimore MD 21218, USA

³ Apple Inc., USA

Abstract. Denoising Diffusion Probabilistic Models (DDPMs) have accomplished much in the realm of generative AI. Despite their high performance, there is room for improvement, especially in terms of sample fidelity by utilizing statistical properties that impose structural integrity, such as isotropy. Minimizing the mean squared error between the additive and predicted noise alone does not impose constraints on the predicted noise to be isotropic. Thus, we were motivated to utilize the isotropy of the additive noise as a constraint on the objective function to enhance the fidelity of DDPMs. Our approach is simple and can be applied to any DDPM variant. We validate our approach by presenting experiments conducted on four synthetic 2D datasets as well as on unconditional image generation. As demonstrated by the results, the incorporation of this constraint improves the fidelity metrics, Precision and Density for the 2D datasets as well as for the unconditional image generation.

Keywords: Generative Models · Diffusion Models · Structure · Image Generation · Gaussian Noise

1 Introduction

Diffusion models have been accomplishing great feats in the realm of generative AI, specifically in terms of unconditional and conditional image generation ([12], [5], [18], [11], [15], [17], [6]). Starting with the revolutionary paper by Ho et al. [4] and the improvements by Nichol et al. [12] as well as the Latent Diffusion Model by Rombach et al. [17], these models have had the biggest impact in this context. The fidelity and diversity of these generated images are surprisingly amazing. Yet, as with all models, these models can still be improved upon closer inspection. As with the improvements done by Nichol et al. [12] to the original Denoising Diffusion Probabilistic Model (DDPM) by introducing techniques such as the cosine-based variance schedule as well as making the model learn the variance rather than keeping it fixed, helped improve the performance of DDPMs. Our goal in this paper is to make a similar contribution with regards to the improvement of the important fidelity metrics, Density [10] and Precision [8].

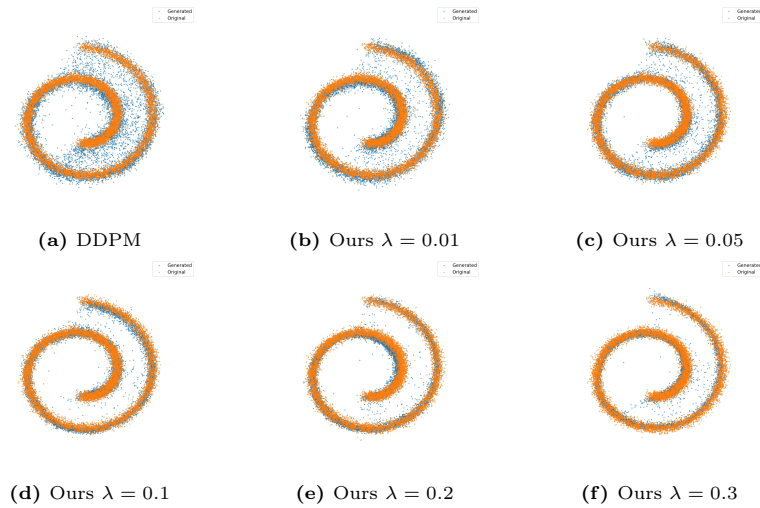


Fig. 1: The variation of the Generated Distribution (in blue) compared to the Ground Truth Distribution (in orange). The plots indicate that the generated samples are much more closely connected and densely packed with the increase of the regularization parameter, λ . The plots show the utility of imposing the isotropy constraint based loss function which enables the generation of more realistic samples as most of generated samples are concentrated near the ground truth samples.

Although DDPMs perform well, we noticed that these existing models do not necessarily incorporate any distributional (structural) information about the particular dataset it tries to generate. Typically, the DDPM's forward process gradually pushes the dataset towards a white gaussian, which can be thought of as a structural vanishing point of the data distribution. This implies a well placed point of origin for the generative process (reverse path) from a point of complete lack of structure towards the final destination which is the data distribution. In the DDPM implementation, the learning process considers the expected squared norm difference between the additive gaussian noise and the predicted noise as its objective function. Therefore, for the generative process, to enhance the aforementioned creation of structure, the objective function can be modified to include any structural measure, such as isotropy. In the context of this paper, "isotropy" describes the affinity towards a white distribution quantified by the expected squared norm of the distribution. However, the objective function in the existing models only focus on the expected squared norm difference between the additive gaussian noise and the predicted noise.

Thus, we were motivated to include the isotropic nature of the additive gaussian noise when optimizing for the objective to further enhance the statistical properties of the predicted noise. Our intuition is that by capturing the statistical properties of the noise in more detail, the model will be able to produce

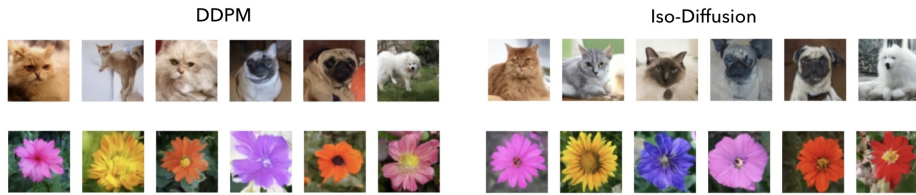


Fig. 2: Comparison of the generated images via the DDPM (left) and Iso-Diffusion (right). The DDPM generated images contain much more artefacts and do not seem realistic. However, the generated images via Iso-Diffusion are much more realistic and thus, they are of high fidelity.

higher fidelity samples as it would have much more information regarding the distributional structure of the samples.

As the rationale for introducing isotropy to the objective function has been established. Now, we let’s see how isotropy establishes convergence and quantifies structural information about the distribution. For example, the isotropy of a white gaussian vector in \mathbb{R}^n is the expected squared norm of that vector, which is equal to its dimension, n [23]. This establishes the upper bound in the limit for a normalized distribution with complete lack of structure, which in other words is white. On the hand, the desired distribution, which has more structure and is more colored, would consequently have a lower isotropy value. This implies that the generative process, in its drive towards a structural distribution minimizes isotropy. Furthermore, when analyzing the mean square error objective, we observed that the isotropic nature of the noise, when included, effectively makes the objective function equal to 0 in expectation.

The inclusion of this constraint does not incur a large computational cost and can be readily applied to any of the diffusion model variants. In this work, we experimented on four 2D synthetic datasets with our modified objective function and show that the fidelity metrics, in particular the Density, improves significantly. This implies that the proposed constraint attempt to latch on to the more information rich dense modes of the desired distribution. Furthermore, we validate our approach on unconditional image generation using the Oxford Flowers [13] and Oxford-IIIT Pet [14] datasets. We compare the fidelity and diversity of the generated samples based on key evaluation metrics such as Precision and Recall [8], Density and Coverage [10], Frechet Inception Distance (FID) [2] and Inception Score (IS) [19].

The contributions of this work are as follows:

- We introduce Iso-Diffusion: a modified approach that introduces an isotropic constraint on the predicted noise objective function to steer the generative process in a structurally coherent manner. This results in improved fidelity of the generated data distribution. We believe, to the best of our knowledge, that we are the first to propose such a modified loss based on the properties of the noise.

- We analyze the simple loss function in the DDPM and its connection to isotropy. Moreover, we show that the isotropy of the data distribution monotonically increases and converges to the maximum isotropy value which corresponds to a white gaussian distribution. This confirms that the definition of isotropy, mentioned in this paper, conveys information about the structural information of the data distribution when the data distribution undergoes the forward process in DDPMs.
- We evaluate and validate our approach on four 2D synthetic datasets as well as on the task of unconditional image generation on Oxford Flowers and Oxford-IIIT Pet datasets. Considering the key evaluation metrics, such as the Precision, Recall, Density, Coverage, FID and IS, the modified objective is able to surpass the original DDPM with a significant gap in terms of the fidelity metrics, Density and Precision.

2 Related Work

Deep Generative Models Generative models (GANs [1], VAEs [7], flow-based models [16], and diffusion models [4]) learn the probability distribution of given data, allowing us to sample new data points from the distribution. Deep generative models have been used for generating images, videos [3], 3d objects [9], etc. Moreover, these models have been used for inverse problem solving [22] and to understanding the latent representations of the distributions.

Diffusion Models Diffusion models, in particular, have been making huge improvements and have been used in many domains due to their high generative capabilities. There are mainly two types of diffusion models, one is the Score based approach introduced by Song and Ermon [21] and the other, which is the focus of this work, is the one introduced by Ho et al. [4]. Both modeling types have been able to achieve state-of-the-art performance in generative modeling tasks and have motivated the growth of many subsequent works in generative models.

Improving Diffusion Models In the context of DDPMs [4], there have been several seminal papers that have contributed to the improvement of these models. In particular, Nichol et al.’s [12] work presented several key insights into how one could improve the training of these models. One such insight is the use of a cosine-based variance schedule rather than the linear variance schedule used by Ho et al. [4]. These changes were able to improve the DDPM further.

However, most of these improvements were focused on improving the models based on the most widely used metrics for image generation, FID and IS. But, some of the recent work ([8], [10]), in generative models have pointed out that FID and IS are not necessarily indicative of the actual fidelity of the samples generated by generative models. Thus, researchers have been focusing on finding other metrics, such as Precision and Density, to assess the fidelity of these generated samples. In particular we observed that the Density takes the local context (measuring how close it is to densely packed samples of the true distribution) of a sample into account during its calculation. We believe that this makes the Density a vital metric to assess the samples’ fidelity.

3 Background

Diffusion probabilistic models were first introduced by Sohl-Dickstein et al. [20]. These models fall under the category of generative models which learn the distribution of the data so that they can sample from these data distributions. However, it wasn't until Ho et al. [4] that Diffusion Probabilistic Models took off. In the next few subsections, we will provide a brief overview of the DDPM definitions that will be useful to understanding our work.

3.1 Definitions

In the DDPM, we simply add a gaussian noise, which varies according to a specific variance schedule, $\beta_t \in (0, 1)$. The noise at each time-step corrupts the data, such that by the time the time-step reaches its final value, T , the data will be mapped to an almost white gaussian distribution. However, the learning occurs when we try to learn the reverse process by which we try to denoise along the same trajectory starting from the almost white gaussian distribution. The first process, in which we add noise, is called the forward process and the latter, in which we denoise, the reverse process. The forward process is often characterized by q and the reverse process by p . Both of which are modeled as gaussian distributions.

The forward process is defined as follows,

$$q(x_1, x_2, \dots, x_T | x_0) = \prod_{t=1}^T q(x_t | x_{t-1}) \quad (1)$$

$$q(x_t | x_{t-1}) \sim \mathcal{N}(x_t; \sqrt{1 - \beta_t} x_{t-1}, \beta_t \mathbf{I}) \quad (2)$$

Moreover, by introducing $\alpha_t = 1 - \beta_t$ as well as $\bar{\alpha}_t = \prod_{i=1}^t \alpha_i$ the forward process can be further simplified into the following expression via the re-parametrization trick [7]. Since,

$$q(x_t | x_{t-1}) \sim \mathcal{N}(x_t; \sqrt{1 - \beta_t} x_{t-1}, \beta_t \mathbf{I}) \quad (3)$$

$$q(x_t | x_0) \sim \mathcal{N}(x_t; \sqrt{\bar{\alpha}_t} x_0, \sqrt{1 - \bar{\alpha}_t} \mathbf{I}) \quad (4)$$

$$x_t = \sqrt{\bar{\alpha}_t} x_0 + \sqrt{1 - \bar{\alpha}_t} \epsilon \quad (5)$$

where, $\epsilon \in \mathcal{N}(0, \mathbf{I})$.

The reverse process, given by $p \sim \mathcal{N}(x_{t-1} | x_t)$, can be obtained in terms of the forward process distribution q and the Baye's Theorem. However, the reverse process only becomes tractable when the posterior distribution $q(x_{t-1} | x_t)$, is conditioned on the input data x_0 . Thus, during training, the model tries to learn the tractable $q(x_{t-1} | x_t, x_0)$ distribution. This distribution, which is also a gaussian distribution, is defined by the following equation and parameters.

$$q(x_{t-1}|x_t, x_0) \sim \mathcal{N}(x_{t-1}; \tilde{\mu}(x_t, x_0), \tilde{\beta}_t \mathbf{I}) \quad (6)$$

$$\tilde{\beta}_t = \frac{1 - \bar{\alpha}_{t-1}}{1 - \bar{\alpha}_t} \beta_t \quad (7)$$

$$\tilde{\mu}_t(x_t, x_0) = \frac{\sqrt{\bar{\alpha}_{t-1}} \beta_t}{1 - \bar{\alpha}_t} x_0 + \frac{\sqrt{\bar{\alpha}_t} (1 - \bar{\alpha}_{t-1})}{1 - \bar{\alpha}_t} x_t \quad (8)$$

3.2 Training Process

To train, however, one could make the model predict the mean of the reverse process distribution at each time step. But, Ho et al. [4] mentions that predicting, the additive noise, ϵ , leads to better results. The additive noise and the mean of the reverse process distribution at each time step are elegantly linked by equations (5) and (8). This results in the following re-parametrization of $\tilde{\mu}(x_t, t)$,

$$\tilde{\mu}(x_t, t) = \frac{1}{\sqrt{\alpha_t}} \left(x_t - \frac{1 - \alpha_t}{\sqrt{1 - \bar{\alpha}_t}} \epsilon \right) \quad (9)$$

Therefore, predicting the additive noise, ϵ , is adequate for the task of predicting the mean of the backward process distribution. Moreover, since the forward process' variance schedule is fixed, the reverse process variance, $\tilde{\beta}_t$, is also assumed to be fixed according to $\tilde{\beta}_t$.

Thus, Ho et al. [4] proposes to optimize the following simple objective function during the training process.

$$L_{\text{simple}} = E_{t, x_0, \epsilon} [\|\epsilon - \epsilon_\theta(x_t, t)\|^2] \quad (10)$$

where, $\epsilon_\theta(x_t, t)$ is the predicted noise.

3.3 Hidden Statistical Properties of ϵ

Upon closer inspection of the L_{simple} objective function, we see that the objective of the U-Net is to minimize the mean squared error between ϵ and ϵ_θ . Yet, if the simple loss is expanded further, a rather informative mathematical expression can be obtained.

$$E[\|\epsilon - \epsilon_\theta\|^2] = E[(\epsilon - \epsilon_\theta)^T (\epsilon - \epsilon_\theta)] \quad (11)$$

$$= E(\epsilon^T \epsilon) + E(\epsilon_\theta^T \epsilon_\theta) - 2E(\epsilon_\theta^T \epsilon) \quad (12)$$

Now, since we know that $\epsilon \sim \mathcal{N}(0, \mathbf{I})$, it is an isotropic distribution. Thus, by definition, since ϵ is an isotropic random vector in \mathbb{R}^n , the expected norm of the random vector, $E(\epsilon^T \epsilon) = n$.

Furthermore, since the goal is to predict the noise as accurately as possible, ϵ_θ should also be distributed according to a white gaussian distribution, i.e.,

$\epsilon_\theta \sim \mathcal{N}(0, \mathbf{I})$. Hence, if ϵ and ϵ_θ are both independent identical isotropic random vectors,

$$E[||\epsilon - \epsilon_\theta||^2] = E(\epsilon^T \epsilon) + E(\epsilon_\theta^T \epsilon_\theta) - 2E(\epsilon_\theta^T \epsilon) \quad (13)$$

$$= n + n - 2n \quad (14)$$

$$= 0 \quad (15)$$

4 Analysis on the Isotropy of x_t

Inspired, we wanted to find out further implications of imposing structural information in the DDPM. As it turns out, we were able to gain more interesting insights about the forward process of the DDPM. For example, if we consider equation (5) and consider the isotropy, expected squared norm of x_t , we see that,

$$E(||x_t||^2) = E(x_t^T x_t) = \bar{\alpha}_t E(x_0^T x_0) + (1 - \bar{\alpha}_t) E(\epsilon^T \epsilon) + 2\sqrt{(\bar{\alpha}_t)(1 - \bar{\alpha}_t)} E(x_0^T \epsilon) \quad (16)$$

However, since ϵ is a white gaussian random vector, it is isotropic. Moreover, by assuming that it is independent of the distribution of x_0 , when x_0 is non-isotropic, we see that,

$$E(x_0^T \epsilon) = 0 \quad (17)$$

Therefore,

$$E(x_t^T x_t) = \bar{\alpha}_t E(x_0^T x_0) + (1 - \bar{\alpha}_t)n \quad (18)$$

$$= n + \bar{\alpha}_t(E(x_0^T x_0) - n) \quad (19)$$

Thus, when the input data are normalized and they are distributed according to a non-isotropic distribution, we note that the maximum of the expected squared norm of x_0 , $E(x_0^T x_0)_{\max} = n$. Hence, $E(x_0^T x_0) - n \leq 0$. Thus, during the forward process, since $\bar{\alpha}_t > 0$, the expected squared norm of x_t can be at most n , $\forall t \in [1, T]$ and attains the maximum value at the final time-step T .

$$E(x_t^T x_t) \leq n \quad (20)$$

Moreover, when we consider two consecutive time steps, t and $t + 1$, we see that,

$$E(x_{t+1}^T x_{t+1}) = n + \bar{\alpha}_{t+1}(E(x_0^T x_0) - n) \quad (21)$$

$$E(x_t^T x_t) = n + \bar{\alpha}_t(E(x_0^T x_0) - n) \quad (22)$$

$$E(x_{t+1}^T x_{t+1}) - E(x_t^T x_t) = (E(x_0^T x_0) - n)(\bar{\alpha}_{t+1} - \bar{\alpha}_t) \quad (23)$$

We know that $E(x_0^T x_0) - n \leq 0$ and that $\bar{\alpha}_{t+1} - \bar{\alpha}_t \leq 0$. Thus,

$$E(x_{t+1}^T x_{t+1}) - E(x_t^T x_t) \geq 0 \quad (24)$$

$$E(x_{t+1}^T x_{t+1}) \geq E(x_t^T x_t) \quad (25)$$

Therefore, for any particular normalized data distribution, we see that during the forward process, the isotropy of the data distribution increases, and finally converges to the isotropy of a white gaussian vector, when the data distribution completely converts into a white gaussian distribution. Hence, the definition of isotropy given in this paper, aligns perfectly with the fact that the isotropy quantifies structural information about the data distribution.

5 Isotropy Based Loss Function

Armed with the above analyses, we proceeded to modify the objective function L_{simple} to include a regularization term which penalizes the model, if the model predicts a noise which is not necessarily isotropic. Hence, the new modified objective function we propose to optimize is,

$$L_{\text{modified}} = E(\|\epsilon - \epsilon_\theta\|^2) + \lambda(E(\epsilon_\theta^T \epsilon_\theta) - n)^2 \quad (26)$$

where λ is the regularization parameter.

However, this modified objective needs to be further simplified so as to make this new error be independent of the size of the dimension of the random vector. Thus, we make the following modification during implementation.

$$L_{\text{modified}} = E(\|\epsilon - \epsilon_\theta\|^2) + \lambda \left(E \left(\frac{\epsilon_\theta^T \epsilon_\theta}{n} \right) - 1 \right)^2 \quad (27)$$

6 Experiments

6.1 Experimental Setup

To validate our approach we consider 2D synthetic data as well as images. For the 2D data, we utilized a conditional dense network consisting of 3 fully-connected hidden layers with ReLU activations. The learning rate was fixed at 1e-3. All the datasets were learned using 1000 time-steps and 1000 epochs.

For the image datasets, we consider the same version of the U-Net utilized in the original DDPM implementation with a learning rate of 2e-4. The U-Net was trained with 1000 time-steps for 1000 epochs as well.

For each dataset, when reporting the metrics, we consider the average of 3 training runs for each of the models. Moreover, all the experiments were run on one Quadro GV-100 GPU with 32GB of VRAM.

6.2 Synthetic Data

For the synthetic generation experiments, we consider four 2D synthetic datasets, namely, the Swiss Roll, the Inter-twining moons, the S-Curve and the 8-gaussians datasets. To evaluate the proposed method, we utilize the most informative generative model metrics, such as the Precision, Recall, Density and Coverage.

Table 1: Comparison of Evaluation Metrics for the two methods : DDPM and Iso-Diffusion for the 2D Datasets

Metrics	Swiss Roll		Moons		S-Curve		8-gaussians	
	DDPM	Ours	DDPM	Ours	DDPM	Ours	DDPM	Ours
Precision	0.90	0.982	0.987	0.991	0.989	0.992	0.994	0.997
Recall	0.998	0.984	0.999	0.997	0.996	0.989	0.997	0.988
Density	0.83	0.989	0.957	0.979	0.978	0.982	0.983	0.989
Coverage	0.895	0.917	0.943	0.938	0.938	0.91	0.932	0.90

Table 2: Metrics Variation with the Regularization Parameter for the Swiss Roll Dataset (λ)

Method	Precision	Recall	Density	Coverage
DDPM ([4])	0.90 (± 0.005)	0.998 (± 0.0001)	0.83 (± 0.02)	0.895 (± 0.025)
Ours $\lambda = 0.01$	0.93 (± 0.022)	0.998 (± 0.0002)	0.885 (± 0.0035)	0.90 (± 0.055)
Ours $\lambda = 0.05$	0.971 (± 0.0009)	0.992 (± 0.0002)	0.955 (± 0.001)	0.92 (± 0.015)
Ours $\lambda = 0.10$	0.982 (± 0.0001)	0.984 (± 0.003)	0.989 (± 0.005)	0.917 (± 0.001)
Ours $\lambda = 0.20$	0.99 (± 0.001)	0.983 (± 0.003)	1.0 (± 0.001)	0.875 (± 0.025)
Ours $\lambda = 0.30$	0.983 (± 0.003)	0.96 (± 0.015)	1.0 (± 0.01)	0.85 (± 0.035)

Of these metrics, Precision and Density measure the fidelity of the generated samples, whereas the Recall and Coverage measure the diversity of the generated samples.

Table 1 summarizes the demonstrated improvements made by our modified loss in terms of these metrics. Across all these datasets we observe that the fidelity metrics, Precision and Density have been improved. Specifically, when considering the Swiss Roll and the Moons datasets, we have been able to achieve much larger improvement in terms of the Density.

The visualized plots of the generated data distributions (figures 1, 3, 4, and 5) indicate that the modified loss function based samples are much more closely gathered and concentrated near the ground-truth data. On the contrary, we can observe that the samples generated via the original DDPM loss function,

Table 3: Metrics Variation with the Regularization Parameter for the Moons Dataset (λ)

Method	Precision	Recall	Density	Coverage
DDPM ([4])	0.987 (± 0.001)	0.999 (± 0.001)	0.957 (± 0.009)	0.943 (± 0.009)
Ours $\lambda = 0.01$	0.980 (± 0.0004)	0.999 (± 0.0008)	0.942 (± 0.0003)	0.926 (± 0.025)
Ours $\lambda = 0.05$	0.985 (± 0.004)	0.998 (± 0.0001)	0.957 (± 0.02)	0.947 (± 0.0045)
Ours $\lambda = 0.10$	0.991 (± 0.001)	0.997 (± 0.001)	0.979 (± 0.0001)	0.938 (± 0.017)
Ours $\lambda = 0.20$	0.995 (± 0.001)	0.991 (± 0.0028)	0.992 (± 0.005)	0.924 (± 0.013)
Ours $\lambda = 0.30$	0.992 (± 0.001)	0.992 (± 0.005)	1.0 (± 0.006)	0.90 (± 0.005)

Table 4: Metrics Variation with the Regularization Parameter for the S-Curve Dataset (λ)

Method	Precision	Recall	Density	Coverage
DDPM ([4])	0.989 (± 0.003)	0.996 (± 0.003)	0.978 (± 0.008)	0.938 (± 0.008)
Ours $\lambda = 0.01$	0.988 (± 0.003)	0.996 (± 0.002)	0.969 (± 0.011)	0.931 (± 0.01)
Ours $\lambda = 0.05$	0.989 (± 0.004)	0.994 (± 0.005)	0.974 (± 0.011)	0.925 (± 0.014)
Ours $\lambda = 0.10$	0.991 (± 0.004)	0.993 (± 0.005)	0.977 (± 0.012)	0.921 (± 0.019)
Ours $\lambda = 0.20$	0.992 (± 0.004)	0.989 (± 0.012)	0.982 (± 0.015)	0.910 (± 0.036)
Ours $\lambda = 0.30$	0.993 (± 0.004)	0.983 (± 0.018)	0.986 (± 0.017)	0.898 (± 0.043)

Table 5: Metrics Variation with the Regularization Parameter for the 8-gaussians Dataset (λ)

Method	Precision	Recall	Density	Coverage
DDPM ([4])	0.994 (± 0.003)	0.997 (± 0.001)	0.983 (± 0.009)	0.932 (± 0.011)
Ours $\lambda = 0.01$	0.995 (± 0.002)	0.997 (± 0.001)	0.982 (± 0.007)	0.936 (± 0.011)
Ours $\lambda = 0.05$	0.995 (± 0.002)	0.996 (± 0.002)	0.983 (± 0.006)	0.931 (± 0.013)
Ours $\lambda = 0.10$	0.996 (± 0.002)	0.995 (± 0.003)	0.986 (± 0.007)	0.924 (± 0.018)
Ours $\lambda = 0.20$	0.996 (± 0.002)	0.992 (± 0.007)	0.988 (± 0.008)	0.918 (± 0.022)
Ours $\lambda = 0.30$	0.997 (± 0.002)	0.988 (± 0.012)	0.989 (± 0.009)	0.90 (± 0.042)

are not concentrated, but are scattered about. We believe that the isotropy based loss function helps the U-Net learn in such a way that the generated distribution does not contain too many samples which are far away from the most densely packed modes of the ground-truth data distribution. This shows that the proposed loss function, enforces the generated samples to contain properties that pushes them to be closely linked to the real data. Thus, we can directly observe an improvement in the Density metric as it measures the sample fidelity. Furthermore, without any structural information during the training process, the original DDPM is not capable of generating samples which capture the densely packed structure of the distribution and hence it is not necessarily concentrated, but is scattered.

6.3 Unconditional Image Generation

For the unconditional image generation task, we experiment with the Oxford flowers dataset and the Oxford-IIIT Pet dataset. The FID and IS, along with the Precision, Recall, Density and Coverage were used to evaluate the quality of the generated samples.

The results of table 6 further confirm the improvements made by our modified loss on the quality of samples. The Density of the generated images have been significantly improved for the two datasets. Moreover, the FID score has been significantly improved in the Oxford Flowers dataset by the proposed method. Although the FID and IS are considered to be the most widely used evaluation

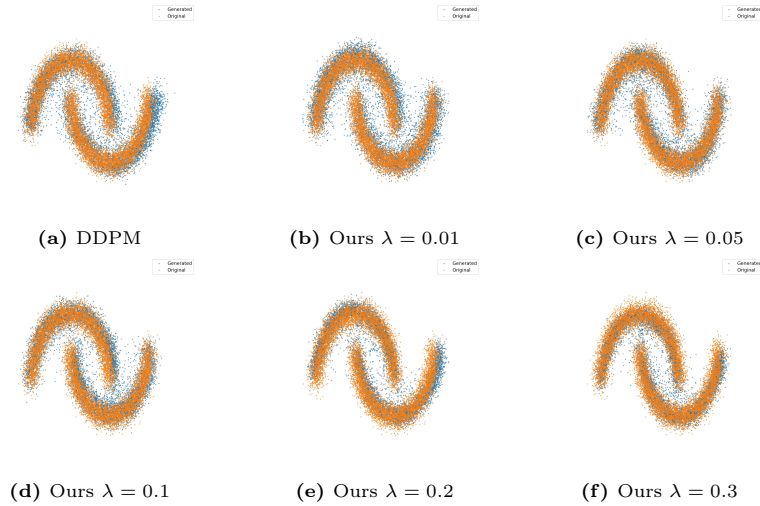


Fig. 3: Variation of the Generated and Ground Truth Distributions with Changing Regularization Parameter Values

metrics for assessing image generation, we see that in the case of the Oxford-IIIT-Pet dataset, they convey little to no discerning information about the generative ability of the proposed method and the original DDPM. But, by using other metrics such as the Precision, Recall, Density and Coverage, we can state that while our proposed method suffers a bit in terms of Recall, the generated samples, see figure 2 are very close to being real as indicated by the improvements in the Precision and Density metrics. Moreover, this is further validated by some of the sample generated by both the original DDPM and the proposed method. The samples generated by the proposed method convey much more realistic characteristics in the images than what can be obtained by using the original DDPM. Thus, this should motivate the research community to propose new evaluation metrics such as Density, which is a much more meaningful measure of fidelity over FID and IS, to assess generative models.

6.4 Variation of the Metrics with the Regularization Parameter

Although the performance of the modified loss function has been able to produce sample which surpass the original DDPM’s samples quality, the quality depends on the regularization parameter of the modified loss function. In particular, we performed a few more experiments by considering a range of values for the regularization parameter.

The metrics for the 2D synthetic datasets with different values of the regularization parameter ranging from 0.01 to 0.30 are tabulated in tables 2, 3, 4, and 5. We see that the fidelity metrics, Precision and Density, gradually improve with the increase of the regularization parameter. On the other hand, however,

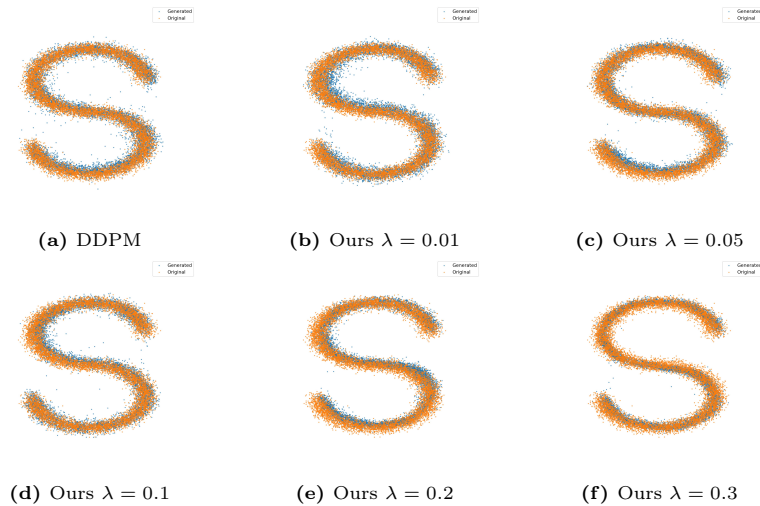


Fig. 4: Variation of the Generated and Ground Truth Distributions with Changing Regularization Parameter Values

we can see that the diversity metrics, Recall and Coverage, gradually decline with the parameter. We believe that this is a direct consequence of imposing a structural constraint on the objective function. It is evident that by focusing on the structure or the isotropy of the distribution, our method is capable of capturing highly dense mode regions and generating samples near them rather than being too diverse. Thus, it increase the fidelity but decreases the diversity of the generated samples.

Table 6: Comparison of Evaluation Metrics for the two Methods in Unconditional Image Generation

Metrics	Oxford Flowers		Oxford-IIIT-Pet	
	DDPM	Iso-Diffusion	DDPM	Iso-Diffusion
FID (\downarrow)	49.60 (± 5.77)	44.77 (± 5.77)	34 (± 0.76)	34.47 (± 0.17)
IS (\uparrow)	3.93 (± 0.12)	3.94 (± 0.12)	12.0 (± 0.27)	12.0 (± 0.27)
Precision (\uparrow)	0.75 (± 0.01)	0.86 (± 0.01)	0.71 (± 0.03)	0.80 (± 0.03)
Recall (\uparrow)	0.21 (± 0.06)	0.14 (± 0.01)	0.29 (± 0.02)	0.24 (± 0.22)
Density (\uparrow)	2.48 (± 0.99)	3.99 (± 0.35)	2.11 (± 0.22)	2.99 (± 0.37)
Coverage (\uparrow)	0.93 (± 0.06)	0.97 (± 0.01)	0.98 (± 0.01)	0.99 (± 0.01)

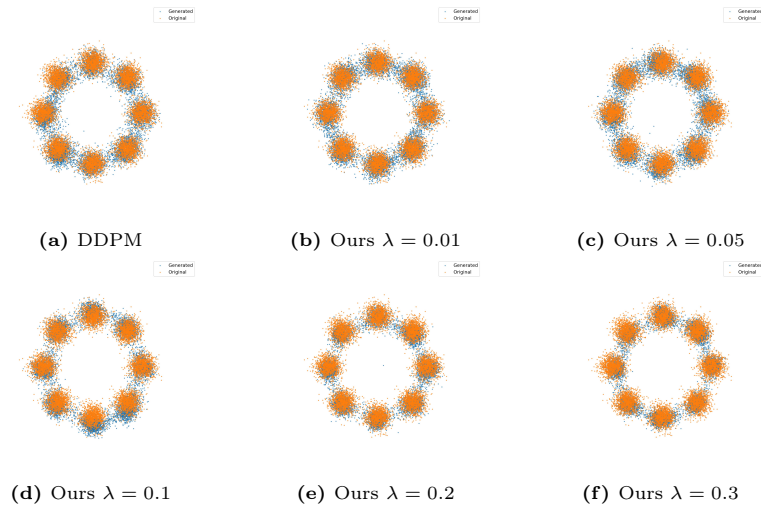


Fig. 5: Variation of the Generated and Ground Truth Distributions with Changing Regularization Parameter Values

7 Conclusion

Denosing Diffusion Probabilistic Models have achieved state-of-the-art performance in generative modeling tasks such as unconditional image generation and image super resolution. However, these models can still be improved upon and much work has been put into improving them. In this paper, we propose another improvement method which is built on the premise that since the distribution that the forward process terminates and the reverse process initiates at a white gaussian distribution, which is isotropic and is void of any structure, it is well motivated, that the incorporation of isotropy as a measure of structure on the loss function will improve the DDPMs’ generated sample fidelity. We, theoretically, show that isotropy is well a defined metric to measure the structure of the distribution during the forward process and the proposed modification helps the DDPM to converge to better solutions based on the simple modified loss. Finally, we validate and show that our modified objective function improves the performance of the DDPM, via experiments performed on 2D synthetic datasets and on unconditional image generation.

References

1. Goodfellow, I., Pouget-Abadie, J., Mirza, M., Xu, B., Warde-Farley, D., Ozair, S., Courville, A., Bengio, Y.: Generative adversarial networks. *Communications of the ACM* **63**(11), 139–144 (2020) [4](#)
2. Heusel, M., Ramsauer, H., Unterthiner, T., Nessler, B., Hochreiter, S.: Gans trained by a two time-scale update rule converge to a local nash equilibrium. *Advances in neural information processing systems* **30** (2017) [3](#)

3. Ho, J., Chan, W., Saharia, C., Whang, J., Gao, R., Gritsenko, A., Kingma, D.P., Poole, B., Norouzi, M., Fleet, D.J., et al.: Imagen video: High definition video generation with diffusion models. arXiv preprint arXiv:2210.02303 (2022) [4](#)
4. Ho, J., Jain, A., Abbeel, P.: Denoising diffusion probabilistic models. *Advances in neural information processing systems* **33**, 6840–6851 (2020) [1](#), [4](#), [5](#), [6](#), [9](#), [10](#)
5. Ho, J., Saharia, C., Chan, W., Fleet, D.J., Norouzi, M., Salimans, T.: Cascaded diffusion models for high fidelity image generation. *The Journal of Machine Learning Research* **23**(1), 2249–2281 (2022) [1](#)
6. Ho, J., Salimans, T.: Classifier-free diffusion guidance. arXiv preprint arXiv:2207.12598 (2022) [1](#)
7. Kingma, D.P., Welling, M.: Auto-encoding variational bayes. arXiv preprint arXiv:1312.6114 (2013) [4](#), [5](#)
8. Kynkäänniemi, T., Karras, T., Laine, S., Lehtinen, J., Aila, T.: Improved precision and recall metric for assessing generative models. *Advances in Neural Information Processing Systems* **32** (2019) [1](#), [3](#), [4](#)
9. Mo, S., Xie, E., Wu, Y., Chen, J., Nießner, M., Li, Z.: Fast training of diffusion transformer with extreme masking for 3d point clouds generation (2023) [4](#)
10. Naeem, M.F., Oh, S.J., Uh, Y., Choi, Y., Yoo, J.: Reliable fidelity and diversity metrics for generative models (2020) [1](#), [3](#), [4](#)
11. Nichol, A., Dhariwal, P., Ramesh, A., Shyam, P., Mishkin, P., McGrew, B., Sutskever, I., Chen, M.: Glide: Towards photorealistic image generation and editing with text-guided diffusion models. arXiv preprint arXiv:2112.10741 (2021) [1](#)
12. Nichol, A.Q., Dhariwal, P.: Improved denoising diffusion probabilistic models. In: *International Conference on Machine Learning*. pp. 8162–8171. PMLR (2021) [1](#), [4](#)
13. Nilsback, M.E., Zisserman, A.: Automated flower classification over a large number of classes. In: *2008 Sixth Indian conference on computer vision, graphics & image processing*. pp. 722–729. IEEE (2008) [3](#)
14. Parkhi, O.M., Vedaldi, A., Zisserman, A., Jawahar, C.V.: Cats and dogs. In: *IEEE Conference on Computer Vision and Pattern Recognition* (2012) [3](#)
15. Ramesh, A., Dhariwal, P., Nichol, A., Chu, C., Chen, M.: Hierarchical text-conditional image generation with clip latents. arXiv preprint arXiv:2204.06125 **1**(2), 3 (2022) [1](#)
16. Rezende, D., Mohamed, S.: Variational inference with normalizing flows. In: *International conference on machine learning*. pp. 1530–1538. PMLR (2015) [4](#)
17. Rombach, R., Blattmann, A., Lorenz, D., Esser, P., Ommer, B.: High-resolution image synthesis with latent diffusion models. In: *Proceedings of the IEEE/CVF conference on computer vision and pattern recognition*. pp. 10684–10695 (2022) [1](#)
18. Saharia, C., Chan, W., Saxena, S., Li, L., Whang, J., Denton, E.L., Ghasemipour, K., Gontijo Lopes, R., Karagol Ayan, B., Salimans, T., et al.: Photorealistic text-to-image diffusion models with deep language understanding. *Advances in Neural Information Processing Systems* **35**, 36479–36494 (2022) [1](#)
19. Salimans, T., Goodfellow, I., Zaremba, W., Cheung, V., Radford, A., Chen, X.: Improved techniques for training gans. *Advances in neural information processing systems* **29** (2016) [3](#)
20. Sohl-Dickstein, J., Weiss, E., Maheswaranathan, N., Ganguli, S.: Deep unsupervised learning using nonequilibrium thermodynamics. In: *International conference on machine learning*. pp. 2256–2265. PMLR (2015) [5](#)
21. Song, Y., Ermon, S.: Generative modeling by estimating gradients of the data distribution. *Advances in neural information processing systems* **32** (2019) [4](#)

22. Song, Y., Shen, L., Xing, L., Ermon, S.: Solving inverse problems in medical imaging with score-based generative models. arXiv preprint arXiv:2111.08005 (2021) [4](#)
23. Vershynin, R.: High-dimensional probability: An introduction with applications in data science, vol. 47. Cambridge university press (2018) [3](#)